Cell Reports, Volume *28*

Supplemental Information

TOM40 Targets Atg2 to Mitochondria-Associated ER Membranes for Phagophore Expansion

Zhenyuan Tang, Yoshinori Takahashi, Haiyan He, Tatsuya Hattori, Chong Chen, Xinwen Liang, Han Chen, Megan M. Young, and Hong-Gang Wang

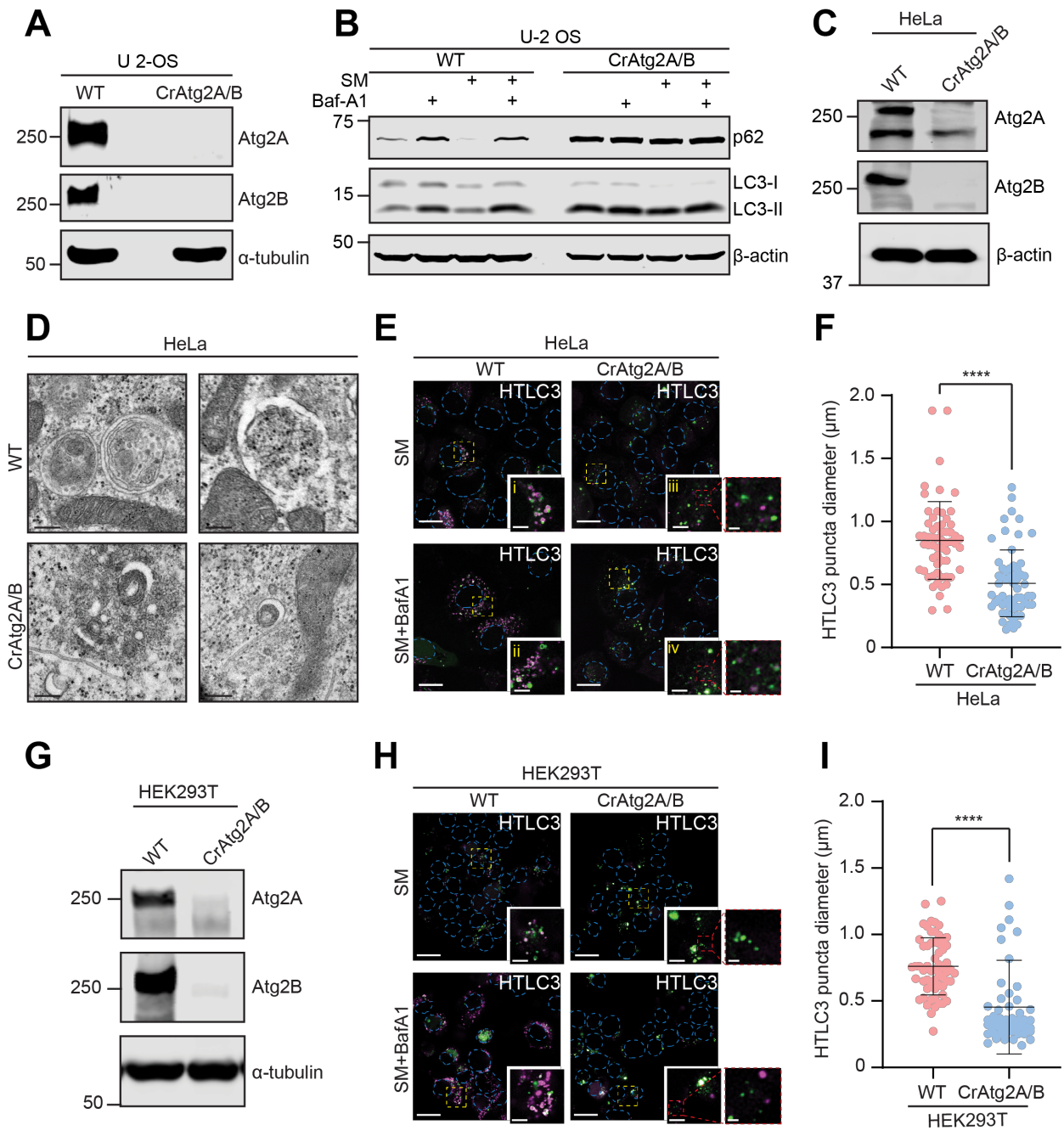
A
U 2-OS
WT
CrAtg2A/B
250
Atg2A
250
Atg2B
50
α-tubulin
B
U-2 OS
WT
CrAtg2A/B
SM
Baf-A1
75
p62
15
LC3-I
LC3-II
50
β-actin
C
HeLa
WT
CrAtg2A/B
250
Atg2A
250
Atg2B
37
β-actin
D
HeLa
WT
CrAtg2A/B
E
HeLa
WT
CrAtg2A/B
SM
SM+BafA1
HTLC3
i
ii
iii
iv
F
****
HTLC3 puncta diameter (μm)
2.0
1.5
1.0
0.5
0
WT
CrAtg2A/B
HeLa
G
HEK293T
WT
CrAtg2A/B
250
Atg2A
250
Atg2B
50
α-tubulin
H
HEK293T
WT
CrAtg2A/B
SM
SM+BafA1
HTLC3
I
****
HTLC3 puncta diameter (μm)
2.0
1.5
1.0
0.5
0
WT
CrAtg2A/B
HEK293T

Figure S1

Figure S1. Loss of Atg2A/B impairs autophagic flux and results in small autophagosomes. Related to Figure 1. (A, C, G) U-2 OS **(A)**, HeLa **(C)**, and HEK293T **(G)** cells were transduced with lentiviruses encoding Cas9 and sgRNAs targeting Atg2A and Atg2B (CrAtg2A/B) and subjected to immunoblotting with the indicated antibodies. **(B)** WT and CrAtg2A/B U-2 OS cells were incubated in complete medium (CM) or starvation medium (SM) for 2 hours in the presence or absence of 100 nM Baf-A1 and subjected to immunoblotting with the indicated antibodies. **(D)** WT and CrAtg2A/B HeLa cells were starved for 2 hours and subjected to transmission electron microscopy. Representative autophagic structures are shown. Red arrowheads indicate autophagic structures. Scale bars represent 200 nm. **(E, H)** HT-LC3-expressing WT and CrAtg2A/B HeLa **(E)** and HEK293T **(H)** cells were incubated in CM or SM in the presence or absence of 100 nM Baf-A1 for 2 hours and subjected to the HT-LC3 autophagosome completion assay followed by confocal microscopy. Magnified images of the boxed areas are shown in the insets (yellow boxes) and the lower bottom right panels (red boxes). Scale bars represent 20 μm, 5 μm (yellow box) and 1 μm (red box) in the magnified images. **(F, I)** The diameters of HT-LC3 foci randomly selected from the starved WT and CrAtg2A/B HeLa **(F)** and HEK293T **(I)** cells were quantified using the Velocity software (n=60). Statistical significance was determined by t-test. All values are mean ± SD. ****$p \leqslant 0.0001$.

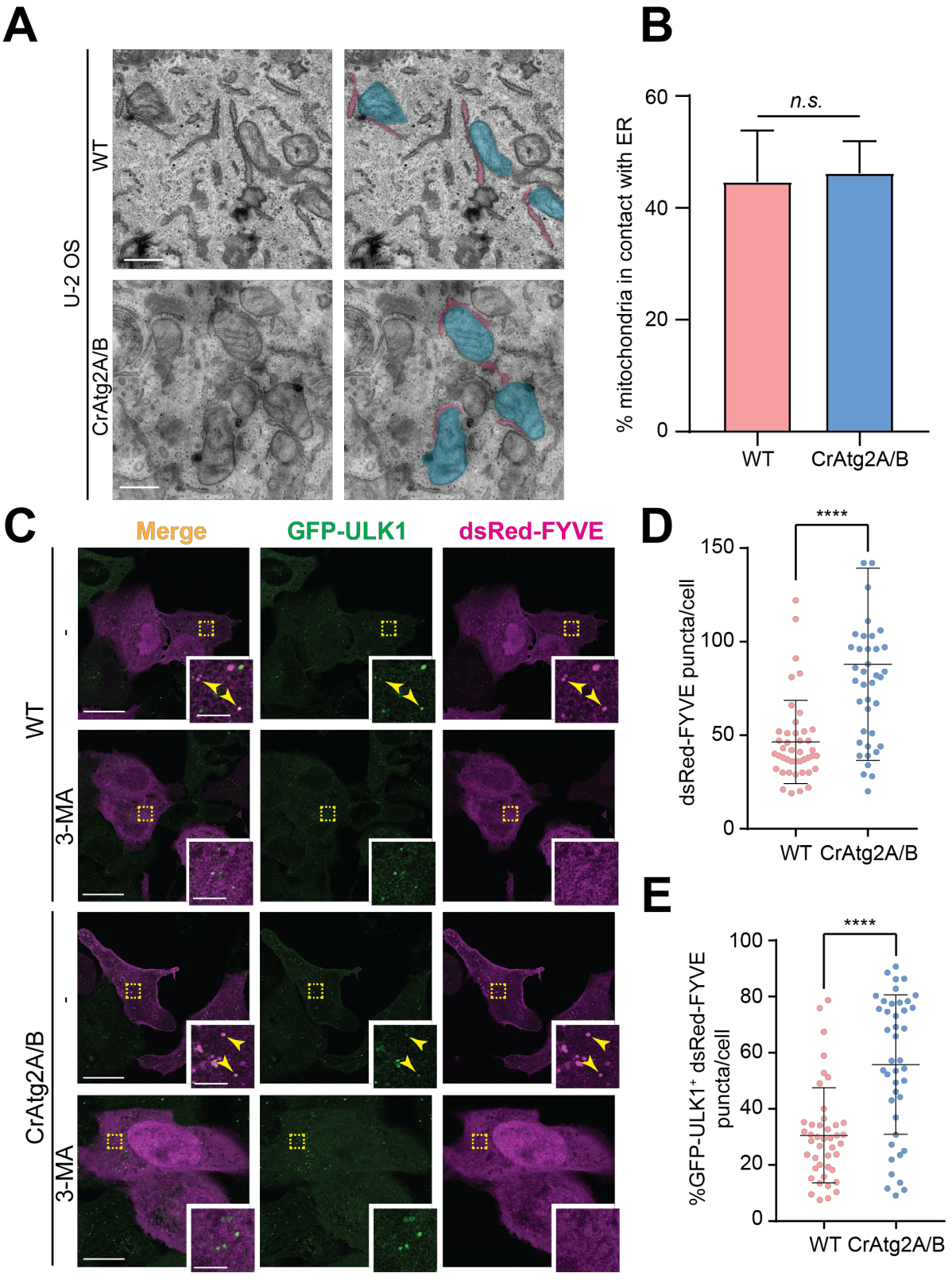
A
U-2 OS
WT
CrAtg2A/B
B
% mitochondria in contact with ER
n.s.
60
40
20
0
WT
CrAtg2A/B
C
Merge
GFP-ULK1
dsRed-FYVE
WT
CrAtg2A/B
-
3-MA
D
dsRed-FYVE puncta/cell
****
150
100
50
0
WT
CrAtg2A/B
E
%GFP-ULK1+ dsRed-FYVE puncta/cell
****
100
80
60
40
20
0
WT
CrAtg2A/B

Figure S2

Figure S2. Atg2A/B is not essential for mitochondria-ER contact site establishment and PI3P distribution. Related to Figure 2. (A) WT and CrAtg2A/B U-2 OS cells were starved for 2 hours and subjected for transmission electron microscopy. Blue and magenta labeled areas represent mitochondria and ER, respectively. Scale bars represent 500 nm. **(B)** The percentage of mitochondria that contact with ER in WT and CrAtg2A/B U-2 OS cells were quantified. (n=1191 mitochondria from 19 WT cells; n=1633 mitochondria from 19 CrAtg2A/B cells). **(C)** GFP-ULK1 stable expressing WT and CrAtg2A/B U-2 OS cells were transiently transfected with dsRed-FYVE for 24 hours, starved in the presence or absence of 10 mM 3-MA for 4 hours, and analyzed by confocal microscopy. Magnified images of the boxed areas are shown in the insets. Scale bars represent 30 μm, and 5 μm in the magnified images. **(D, E)** Total dsRed-FYVE puncta **(D)** and the percentage of GFP-ULK1-positive dsRed-FYVE puncta **(E)** per cell in WT and CrAtg2A/B U-2 OS cells were quantified (n=42). Statistical significance was determined by t-test. All values are mean ± SD. *n.s.* not significant. ****$p \leqslant 0.0001$.

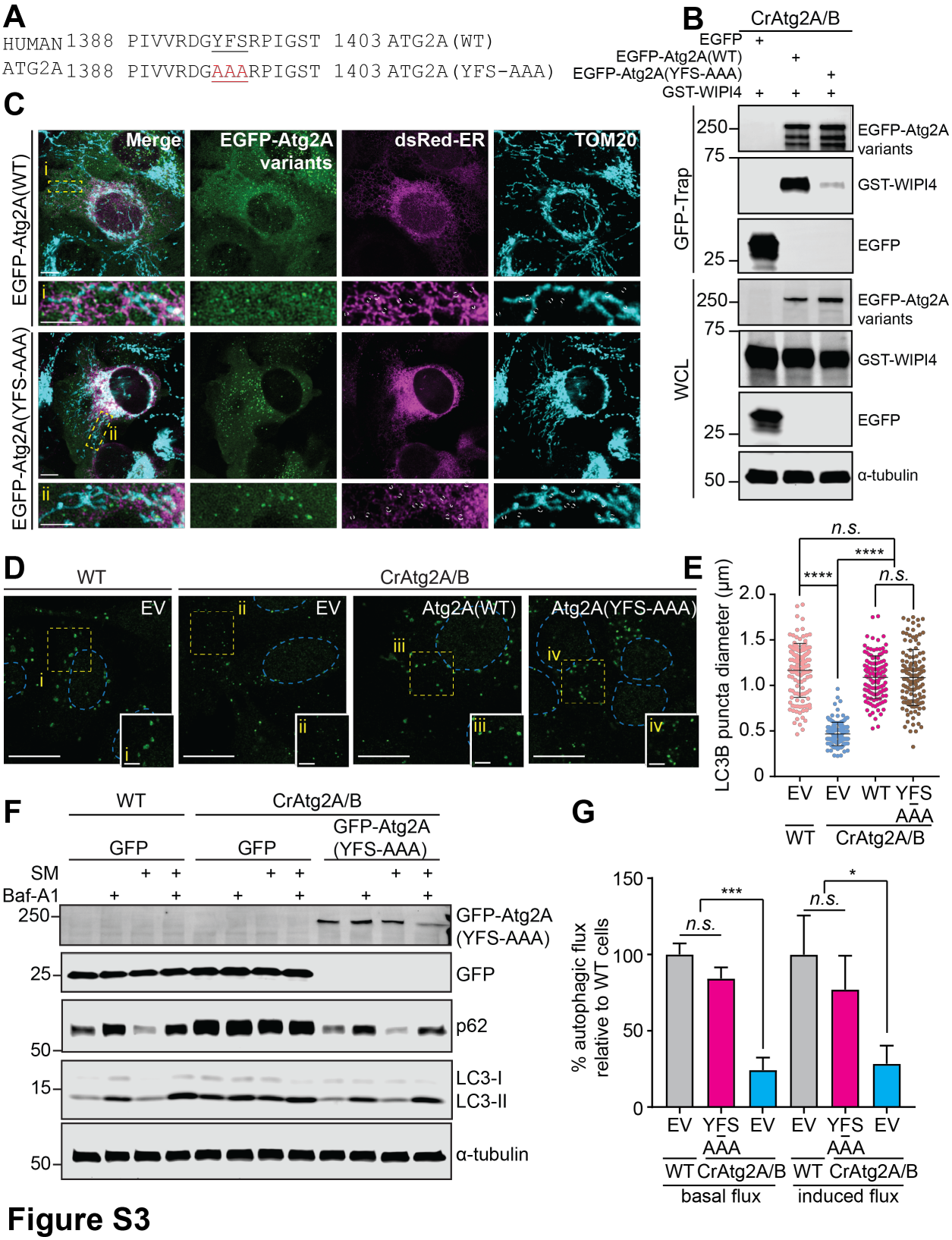
A
HUMAN ATG2A 1388 PIVVRDGYFSRPIGST 1403 ATG2A(WT)
ATG2A 1388 PIVVRDGAAARPIGST 1403 ATG2A(YFS-AAA)
B
CrAtg2A/B
EGFP +
EGFP-Atg2A(WT) +
EGFP-Atg2A(YFS-AAA) +
GST-WIPI4 + + +
GFP-Trap
WCL
250
75
25
50
EGFP-Atg2A variants
GST-WIPI4
EGFP
α-tubulin
C
EGFP-Atg2A(WT)
EGFP-Atg2A(YFS-AAA)
Merge
EGFP-Atg2A variants
dsRed-ER
TOM20
D
WT
CrAtg2A/B
EV
Atg2A(WT)
Atg2A(YFS-AAA)
E
LC3B puncta diameter (μm)
n.s.
****
EV EV WT YFS AAA
WT CrAtg2A/B
F
WT
CrAtg2A/B
GFP
GFP-Atg2A (YFS-AAA)
SM
Baf-A1
GFP-Atg2A (YFS-AAA)
GFP
p62
LC3-I
LC3-II
α-tubulin
G
% autophagic flux relative to WT cells
***
*
EV YFS AAA EV EV YFS AAA EV
WT CrAtg2A/B WT CrAtg2A/B
basal flux
induced flux

Figure S3

Figure S3. The interaction of Atg2A with WIPI4 is dispensable for both autophagosome formation and autophagic flux. Related to Figure 2. (A) The amino acid sequence of the WIPI4 interacting region of Atg2A is shown. The mutated region and substituted amino acids are indicated by underlines and red characters. **(B)** CrAtg2A/B HEK293T cells were transfected with the indicated plasmids for 24 hours and subjected to immunoprecipitation with GFP-Trap beads followed by immunoblotting with the indicated antibodies. **(C)** CrAtg2A/B U-2 OS cells stably expressing dsRed-ER and the indicated EGFP-Atg2A variant were starved for 2 hours, stained for TOM20 and analyzed by confocal microscopy. The magnified images in the boxed areas are shown in the lower panels. Scale bars represent 10 μm, and 5 μm in the magnified images. **(D)** CrAtg2A/B cells U2-OS cells stably expressing the indicated EGFP-Atg2A variants were starved for 2 hours, stained for LC3 and analyzed by confocal microscopy. Magnified images in the boxed areas are shown in the insets. Scale bars represent 20 μm, and 5 μm in the magnified images. EV, WT, YFS represent EGFP-empty vector, EGFP-Atg2A(WT), EGFP-Atg2A(YFS), respectively. **(E)** The diameters of LC3 foci were randomly selected and quantified using the Velocity software (n=130). EV, WT, YFS represent EGFP-empty vector, EGFP-Atg2A(WT), EGFP-Atg2A(YFS), respectively. **(F, G)** The indicated U-2 OS cells were incubated in CM or SM for 2 hours in the presence or absence of 100 nM Baf-A1 and subjected to immunoblotting with the indicated antibodies **(F)**. Basal and starvation-induced autophagic flux in the indicated U-2 OS stable transductants were quantified as described in the Methods (n=3) **(F)**. Statistical significance was determined by one-way ANOVA followed by Dunn's multiple comparisons test. All values are mean ± SD. *n.s.* not significant. *$p \leqslant 0.05$; ***$p \leqslant 0.001$; ****$p \leqslant 0.0001$.

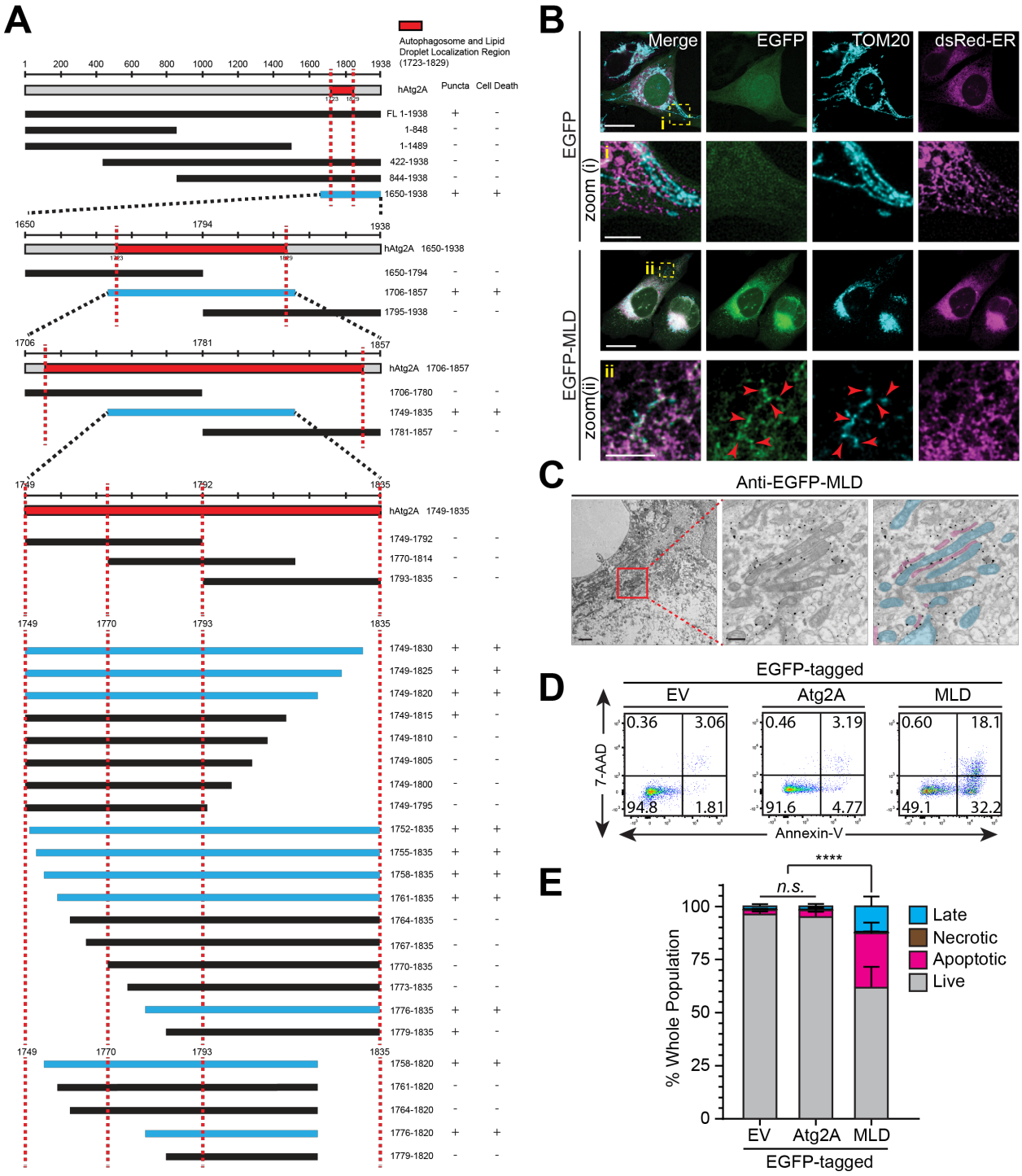
A
Autophagosome and Lipid Droplet Localization Region (1723-1829)
Puncta
Cell Death
hAtg2A
FL 1-1938
1-848
1-1489
422-1938
844-1938
1650-1938
hAtg2A 1650-1938
1650-1794
1706-1857
1795-1938
hAtg2A 1706-1857
1706-1780
1749-1835
1781-1857
hAtg2A 1749-1835
1749-1792
1770-1814
1793-1835
1749-1830
1749-1825
1749-1820
1749-1815
1749-1810
1749-1805
1749-1800
1749-1795
1752-1835
1755-1835
1758-1835
1761-1835
1764-1835
1767-1835
1770-1835
1773-1835
1776-1835
1779-1835
1758-1820
1761-1820
1764-1820
1776-1820
1779-1820
B
Merge
EGFP
TOM20
dsRed-ER
EGFP
zoom (i)
EGFP-MLD
zoom(ii)
C
Anti-EGFP-MLD
D
EGFP-tagged
EV
Atg2A
MLD
7-AAD
Annexin-V
0.36
3.06
94.8
1.81
0.46
3.19
91.6
4.77
0.60
18.1
49.1
32.2
E
****
n.s.
% Whole Population
Late
Necrotic
Apoptotic
Live
EV
Atg2A
MLD
EGFP-tagged

Figure S4

Figure S4. Atg2A(1776-1820) is sufficient for MAM localization. Related to Figure 3. (A) EGFP-tagged human Atg2A was truncated from N- and/or C-terminus sequentially. CrAtg2A/B HEK293T cells were transiently transfected with Atg2A mutants for 24 hours. Cytosolic EGFP-Atg2A mutant punctuation and cell death were analyzed by fluorescence microscopy. The red box represents the previously identified autophagosome and lipid localization region on human Atg2A (AK Velikkakath et al, MBoC, 2012). **(B)** Schematic illustration of MAM localization domain (MLD) of Atg2A. **(C)** CrAtg2A/B U-2 OS cells stably expressing dsRed-ER were transiently transfected with EGFP or EGFP-MLD and subjected to immunofluorescence confocal microscopy using anti-TOM20 antibody. Magnified images in the boxed areas are shown in the lower panels. Scale bars represent 20 μm, and 5 μm in the magnified images. **(D, E)** CrAtg2A/B U-2 OS cells were transiently transfected with EGFP or EGFP-MLD and subjected to immunoelectron microscopy using anti-GFP antibody (**D**) or Annexin-V and 7-AAD staining and flow cytometry analysis (**E**). The magnified image (red box) is shown on the right panel. Blue and magenta labeled areas represent mitochondria and ER, respectively. Scale bars represent 2000 nm, 500 nm in the magnified image **(D)**. Statistical significance was determined by one-way ANOVA followed by Dunn's multiple comparisons test. All values are mean ± SD. *n.s.* not significant. ****$p \leqslant 0.0001$.

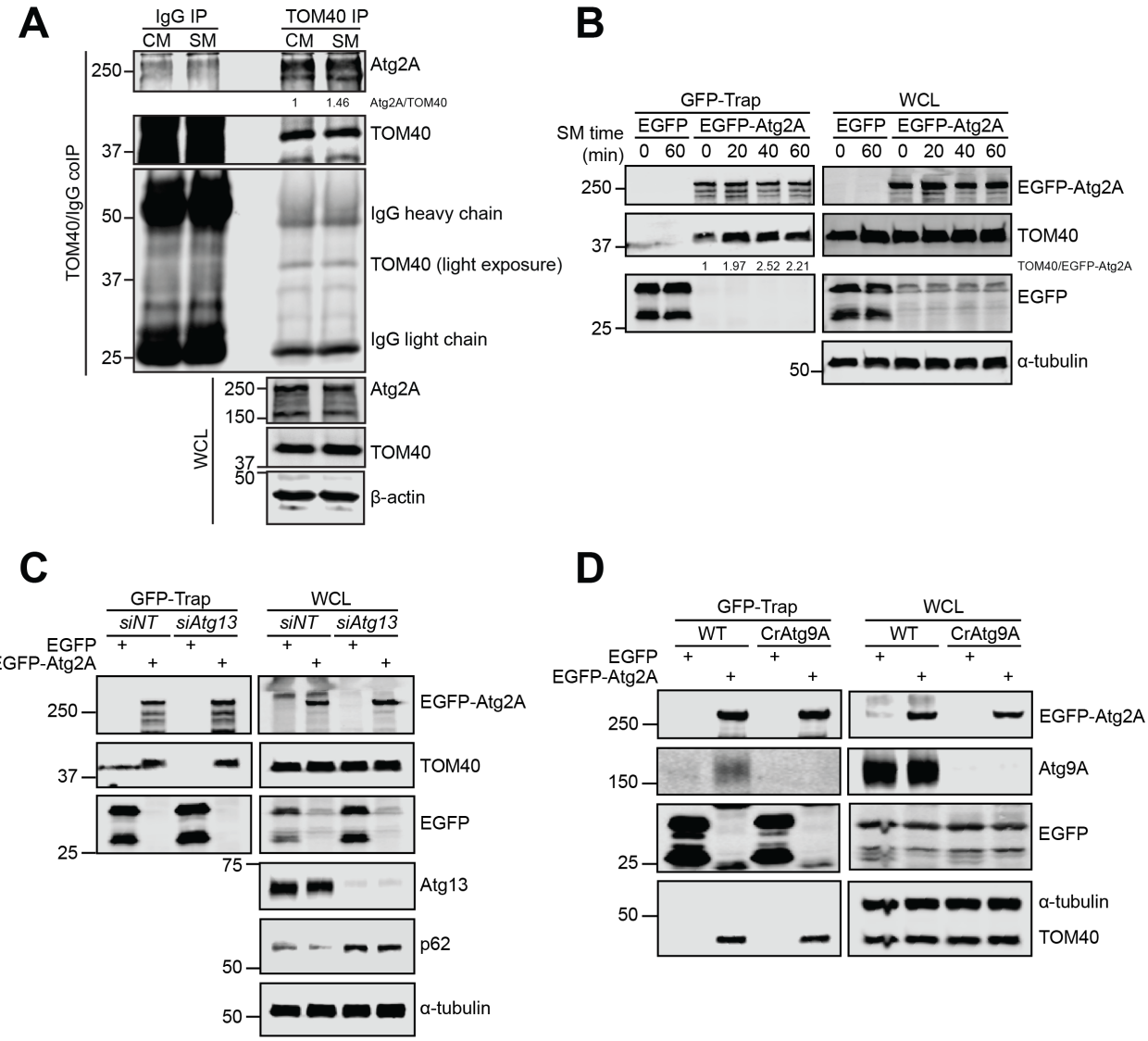
A
IgG IP
TOM40 IP
CM
SM
CM
SM
250
Atg2A
1
1.46
Atg2A/TOM40
37
TOM40
TOM40/IgG coIP
50
IgG heavy chain
37
TOM40 (light exposure)
25
IgG light chain
WCL
250
150
Atg2A
37
TOM40
50
β-actin
B
GFP-Trap
WCL
SM time (min)
EGFP
EGFP-Atg2A
EGFP
EGFP-Atg2A
0
60
0
20
40
60
0
60
0
20
40
60
250
EGFP-Atg2A
37
TOM40
1
1.97
2.52
2.21
TOM40/EGFP-Atg2A
25
EGFP
50
α-tubulin
C
GFP-Trap
WCL
siNT
siAtg13
siNT
siAtg13
EGFP
EGFP-Atg2A
250
EGFP-Atg2A
37
TOM40
25
EGFP
75
Atg13
p62
50
50
α-tubulin
D
GFP-Trap
WCL
WT
CrAtg9A
WT
CrAtg9A
EGFP
EGFP-Atg2A
250
EGFP-Atg2A
150
Atg9A
EGFP
25
50
α-tubulin
TOM40

Figure S5

Figure S5. Atg2A-TOM40 interaction is enhanced by starvation but does not require upstream ATG machinery. Related to Figure 3. **(A)** WT HEK293T cells were incubated in CM or SM for 1 hour and subjected to immunoprecipitation with control IgG or TOM40 antibody followed by immunoblotting with the indicated antibodies. **(B)** CrAtg2A/B HEK293T cells were transfected with EGFP or EGFP-Atg2A for 24 hours and incubated in SM for the indicated time prior to immunoprecipitation with GFP-Trap and followed by immunoblotting with the indicated antibodies. **(C)** CrAtg2A/B HEK293T cells were transfected with non-targeting (siNT) or Atg13 (siAtg13) siRNA for 48 hours followed by EGFP or EGFP-Atg2A transfection for 24 hours prior to immunoprecipitation with GFP-Trap and followed by immunoblotting with the indicated antibodies. **(D)** WT and CrAtg9A HEK293T cells were transfected with EGPF or EGFP-Atg2A for 24 hours and subjected to immunoprecipitation with GFP-Trap and followed by immunoblotting with the indicated antibodies.

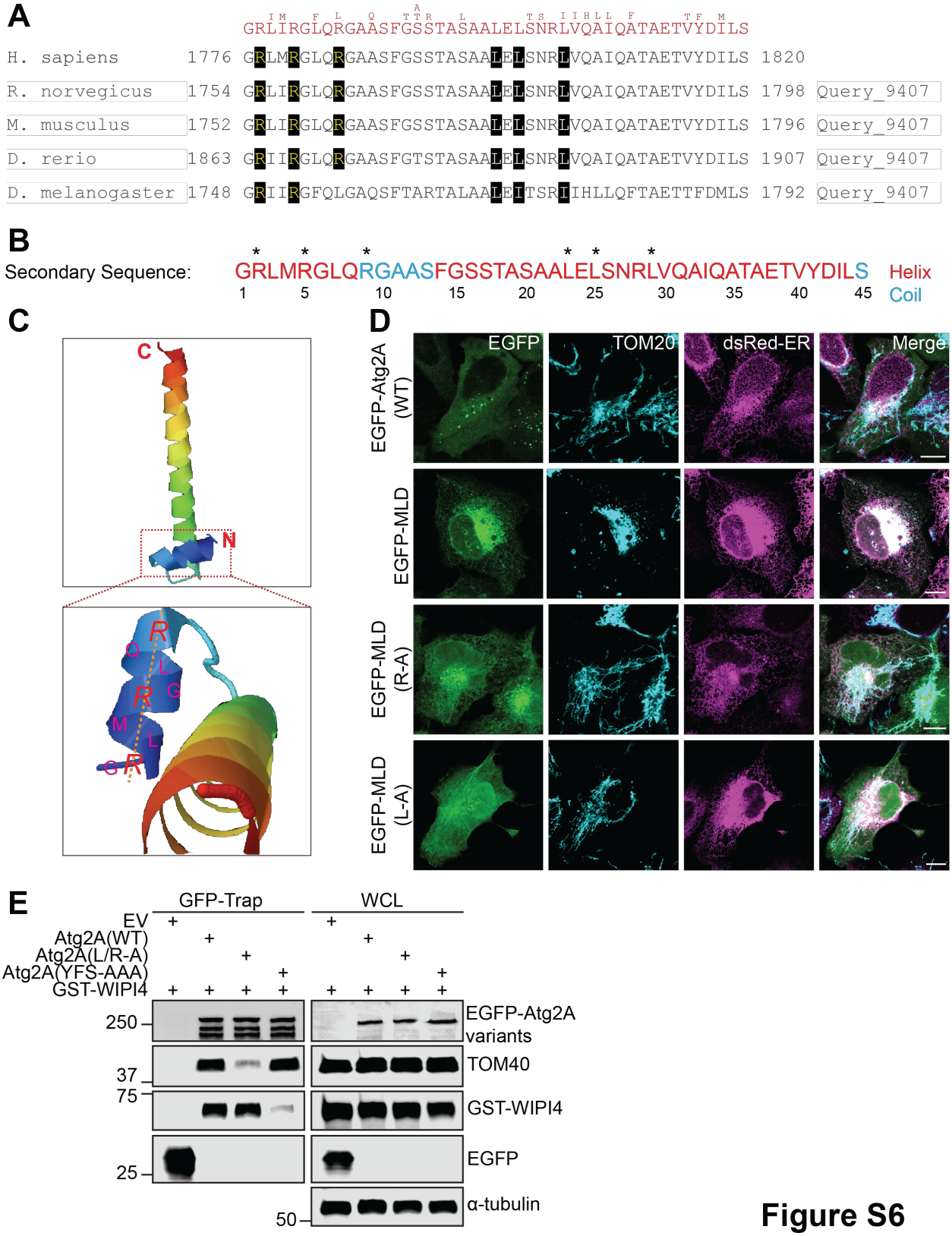
A
GRLIRGLQRGAASFGSSTASAALELSNRLVQAIQATAETVYDILS
H. sapiens 1776 GRLMRGLQRGAASFGSSTASAALELSNRLVQAIQATAETVYDILS 1820
R. norvegicus 1754 GRLIRGLQRGAASFGSSTASAALELSNRLVQAIQATAETVYDILS 1798 Query_9407
M. musculus 1752 GRLIRGLQRGAASFGSSTASAALELSNRLVQAIQATAETVYDILS 1796 Query_9407
D. rerio 1863 GRIIRGLQRGAASFGTSTASAALELSNRLVQAIQATAETVYDILS 1907 Query_9407
D. melanogaster 1748 GRIIRGFQLGAQSFTARTALAALEITSRIIHLLQFTAETTFDMLS 1792 Query_9407
B
Secondary Sequence: GRLMRGLQRGAASFGSSTASAALELSNRLVQAIQATAETVYDILS
1 5 10 15 20 25 30 35 40 45
Helix
Coil
C
C
N
D
EGFP
TOM20
dsRed-ER
Merge
EGFP-Atg2A (WT)
EGFP-MLD
EGFP-MLD (R-A)
EGFP-MLD (L-A)
E
GFP-Trap
WCL
EV
Atg2A(WT)
Atg2A(L/R-A)
Atg2A(YFS-AAA)
GST-WIPI4
250
37
75
25
50
EGFP-Atg2A variants
TOM40
GST-WIPI4
EGFP
α-tubulin

Figure S6

Figure S6. The arginine and leucine residues are crucial for MLD localization. Related to Figure 3. (A) Protein sequence alignment of Atg2A MLD among higher eukaryotes. **(B, C)** Protein secondary (**B**) and tertiary (**C**) structures of MLD were predicted using QUARK ab initio protein structure prediction. Asterisks in **B** indicate the identified crucial amino acid residues for MLD localization. **(D)** dsRed-ER-expressing CrAtg2A/B U2-OS cells were transfected with the indicated EGFP-tagged wild-type or mutant Atg2A for 24 hours, stained for TOM20 and analyzed by confocal microscopy. Scale bars represent 10 μm. **(E)** CrAtg2A/B HEK293T cells were transfected with the indicated plasmids for 24 hours and subjected to immunoprecipitation with GFP-Trap beads followed by immunoblotting with the indicated antibodies.

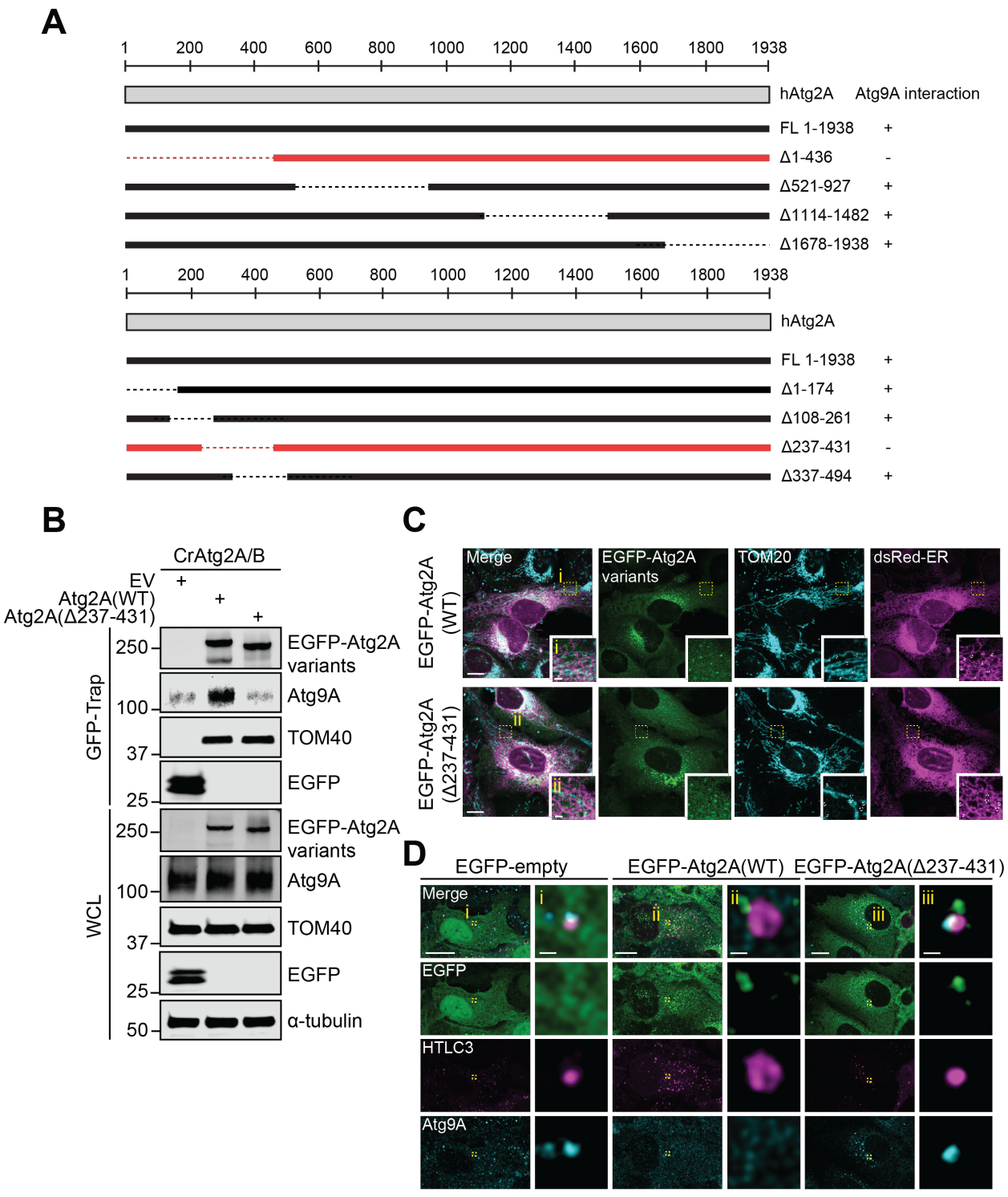
A
1 200 400 600 800 1000 1200 1400 1600 1800 1938
hAtg2A
Atg9A interaction
FL 1-1938 +
Δ1-436 -
Δ521-927 +
Δ1114-1482 +
Δ1678-1938 +
1 200 400 600 800 1000 1200 1400 1600 1800 1938
hAtg2A
FL 1-1938 +
Δ1-174 +
Δ108-261 +
Δ237-431 -
Δ337-494 +
B
CrAtg2A/B
EV
Atg2A(WT)
Atg2A(Δ237-431)
GFP-Trap
WCL
250
100
37
25
50
EGFP-Atg2A variants
Atg9A
TOM40
EGFP
α-tubulin
C
EGFP-Atg2A (WT)
EGFP-Atg2A (Δ237-431)
Merge
EGFP-Atg2A variants
TOM20
dsRed-ER
D
EGFP-empty
EGFP-Atg2A(WT)
EGFP-Atg2A(Δ237-431)
Merge
EGFP
HTLC3
Atg9A

Figure S7

Figure S7. Atg2A is dispensable for the anterograde trafficking of Atg9A. Related to Figure 7. (A) EGFP-tagged human Atg2A was truncated as indicated. Co-immunoprecipitation analyses were performed using GFP-Trap beads to determine the interaction of the indicated Atg2A mutants with Atg9A. **(B)** CrAtg2A/B HEK293T cells were transfected with EGFP-Atg2A variants for 24 hours and subjected to immunoprecipitation with GFP-Trap beads followed by immunoblotting with the indicated antibodies. **(C, D)** CrAtg2A/B U-2 OS cells stably expressing the indicated plasmids were starved for 2 hours, stained for TOM20 (**C**) or Atg9A and MPL (TMR) (**D**) and analyzed by confocal microscopy. Magnified images in the boxed areas are shown in the insets (**C**) and right panels (**D**). Scale bars represent 20 μm, 2.5 μm in the insets in **C**, and 0.5 μm in the magnified images in **D**.

Table S1. List of EGFP-MLD interacting partner candidates. Related to Figure 3. Protein hits are normalized to their corresponding EGFP- or EGFP-MLD peptide number. All candidates, with over 5-fold enrichment, are listed.

	EGFP	EGFP-MLD	EGFP	EGFP-MLD		
gene name	# of peptides		normalize to bait		relative fold-change	Subcellular Localization
EGFP	604	1485				
PHB	11	186	0.01821192	0.12525253	6.877502296	Mit inner
EMC1	5	142	0.00827815	0.0956229	11.55124579	ER
IMMT	3	104	0.00496689	0.07003367	14.10011223	Mit inner
ATAD3B	5	66	0.00827815	0.04444444	5.368888889	Mit inner
TOMM40	2	59	0.00331126	0.03973064	11.9986532	Mit outer
GOLGA5		44	0	0.02962963		Golgi
ALDH3A2	3	41	0.00496689	0.02760943	5.558698092	ER
FAF2	3	38	0.00496689	0.02558923	5.151964085	ER
SAMM50		38	0	0.02558923		Mit outer
RAB3GAP1		34	0	0.02289562		Others
TMEM43	2	31	0.00331126	0.02087542	6.304377104	ER
CHCHD3	1	29	0.00165563	0.01952862	11.7952862	Mit inner
ANKLE2	1	28	0.00165563	0.01885522	11.38855219	ER
MMGT1	1	27	0.00165563	0.01818182	10.98181818	ER
AKAP1		27	0	0.01818182		Mit outer
ZMPSTE24	1	25	0.00165563	0.01683502	10.16835017	ER
TOR1AIP2	1	25	0.00165563	0.01683502	10.16835017	ER
LEMD3		26	0	0.01750842		Nucleus
DNAJC11		26	0	0.01750842		Mit outer
MTX2		24	0	0.01616162		Mit outer
EMC3	1	23	0.00165563	0.01548822	9.354882155	ER
CLCC1	1	23	0.00165563	0.01548822	9.354882155	ER
DNM1L	1	22	0.00165563	0.01481481	8.948148148	Mit outer
ARFGAP1	1	19	0.00165563	0.01279461	7.727946128	Mit outer
ATP2C1		19	0	0.01279461		Golgi
FKBP8	1	18	0.00165563	0.01212121	7.321212121	Mit outer
GOSR1		19	0	0.01279461		Golgi
EPHX1	1	18	0.00165563	0.01212121	7.321212121	ER
FAM114A2		18	0	0.01212121		Nucleus
SPAG9	1	17	0.00165563	0.01144781	6.914478114	Nucleus
TM9SF3	1	17	0.00165563	0.01144781	6.914478114	Others
SPTLC2		18	0	0.01212121		ER
EMC8	1	17	0.00165563	0.01144781	6.914478114	ER

ATP13A1		18	0	0.01212121		ER
CENPH		17	0	0.01144781		Nucleus
SEC24B	1	16	0.00165563	0.01077441	6.507744108	Others
MARCH5		17	0	0.01144781		ER Mit outer
GHDC	1	16	0.00165563	0.01077441	6.507744108	ER
ESYT2	1	16	0.00165563	0.01077441	6.507744108	ER
COMT		17	0	0.01144781		Others
ABHD12		17	0	0.01144781		Others
TMEM205		16	0	0.01077441		Others
MTCH2	1	15	0.00165563	0.01010101	6.101010101	Mit inner
DHRS7		16	0	0.01077441		Others
DHRS7		16	0	0.01077441		Others
SYAP1		15	0	0.01010101		Others
STIM1	1	14	0.00165563	0.00942761	5.694276094	ER
PEX19	1	13	0.00165563	0.00875421	5.287542088	Peroxisome
STXBP3		14	0	0.00942761		Others
STX5	1	13	0.00165563	0.00875421	5.287542088	Golgi
SOAT1		14	0	0.00942761		ER
TPD52L2	1	13	0.00165563	0.00875421	5.287542088	Others
OSBPL9	1	13	0.00165563	0.00875421	5.287542088	Golgi
EMC4		14	0	0.00942761		ER
AAAS		14	0	0.00942761		Nucleus
CAMLG		13	0	0.00875421		ER
NDC1		13	0	0.00875421		Nucleus
ATP6V0A1		13	0	0.00875421		Others
SURF4		13	0	0.00875421		ER
SLC27A4		13	0	0.00875421		ER
MCU		13	0	0.00875421		Mit inner
OSBPL8		13	0	0.00875421		ER
OCIAD1		13	0	0.00875421		Endosome
DIABLO		13	0	0.00875421		Mit outer
ATP6V0D1		13	0	0.00875421		Others
CHCHD6		12	0	0.00808081		Mit inner
ATP2B4		12	0	0.00808081		Others
QSOX2		12	0	0.00808081		Nucleus
MOSPD2		12	0	0.00808081		Others
SNAP29		12	0	0.00808081		Golgi
TDRKH		12	0	0.00808081		Mit outer
LNPK		12	0	0.00808081		ER
NUP210		12	0	0.00808081		ER
MCL1		12	0	0.00808081		Mit outer
CDKAL1		12	0	0.00808081		ER